

EXTRACTION OF THE POROSITY AND PERMEABILITY FOR SMALL PLUGS

Jianlei Sun, Shameem Siddiqui and M. Rafiqul Awal
Texas Tech University, Lubbock, TX, USA

This paper was prepared for presentation at the International Symposium of the Society of Core Analysts held in Austin, Texas, USA 18-21 September, 2011

ABSTRACT

In this paper, we report the findings of a set of standard petrophysical measurements conducted on six core plugs representing limestone, dolomite and sandstone formations and compare them with measurements on several large cutting sized samples derived from these same samples. The tests include absolute and relative permeability, heterogeneity, and petrophysical image analysis of thin sections derived from the samples. We used a CT-based evaluation technique for characterizing heterogeneity in core plugs and large cutting size samples using an inter-slice heterogeneity parameter, an intra-slice heterogeneity parameter and a composite heterogeneity index. The heterogeneity measurements showed one-to-one correspondence between these two sizes showing the potential of the CT-based technique for characterizing heterogeneity. Porosities and absolute permeabilities of core plugs were compared with their corresponding large cutting size samples and generally good agreement was observed between the two scales for the Berea core plugs. Porosities derived from the thin sections of end pieces of each core plug using *ImageJ* also showed good matches with the core analysis based data. CT-based image subtraction technique was also successfully performed to facilitate the steady-state relative permeability measurement for small cutting size samples.

INTRODUCTION

Petrophysical parameters such as porosity and permeability measured in the laboratory are important in understanding multiphase flow processes in porous media. Recent advances in extraction of representative networks from Micro-CT images of drill cuttings and their use in Lattice-Boltzmann or pore network models has led to obtaining some of these petrophysical parameters without coring. However, the data predicted by these models needs to be validated against reliable lab data generated using the same samples at a similar length scale. Siddiqui et al. [1] compared various techniques for measuring density and porosity of cutting-size samples generated from core plugs. Recently Lenormand [2] made an extensive review of existing techniques for measuring permeability on small samples and identified range and domain of applications for techniques for open surface, resin disc and mini-plug categories. Among them, the resin disc method shows strong potential to be used for a wide range of permeabilities from the nano-darcy range to several darcies, and for a sample size larger than 5 mm. Most importantly, the resin disk plate makes it possible to perform conventional relative permeability (K_r) measurements in that it is handily mounted into a regular coreholder.

The uncertainties associated with this method are mainly due to small pore volume, displacement rate sensitivity and capillary end effects. Any method that addresses these issues is going to be very helpful in the validation process involving small samples. Olafuyi et al. [3] conducted relative permeability and capillary pressure experiments on core plugs with bulk volumes ranging from 0.5 to 12 cm³ and concluded that homogeneous samples commonly used to experimentally validate micro-CT network model predictions are sufficiently representative of the larger core scale. There is a strong need to consider the statistical features or patterns due to heterogeneity in order to compare core plug and cutting samples at different scales.

The objective of this paper is to demonstrate a set of procedures that can be used to conduct permeability and relative permeability tests on large cutting-size samples and compare them against data on their larger supersets. The other objective is to compare the heterogeneities of large and small samples and to come up with a better way to measure relative permeabilities of very small core samples.

PROCEDURES

A total of six regular-size core samples were selected to represent the major lithologies – sandstone, dolomite and limestone. Out of these, three are dolomites (from the Permian Basin, DOL01, DOL02 and DOL03), one is a limestone (Bethany limestone, LST01), and two are Berea sandstone (SST01 and SST02). Tests were first conducted on all the core plugs for porosity, absolute and relative permeabilities (unsteady state method) using a standard core flooding apparatus at ambient conditions and at 200 psi back pressure with a 1000 psi confining pressure. The samples were also scanned with a multislice-capable medical CT (computerized tomography) scanner followed by thin section preparation for two end trims of each original core plug. After that, three large cutting size samples (14~21 mm in length, and 8.6~9.0 mm in diameter) were drilled out of each core plug using different orientations - one axial (denoted by the suffix H) and two radial (denoted by suffixes AT and AB, for top and bottom, respectively). This is shown in Figure 1. After that these large cutting size samples were embedded into resin disks of 1-½ inches diameter following the procedure outlined below. The encased samples were then mounted inside a regular core holder and were used in CT-assisted core flooding tests.

Resin encasing procedure

The resin encasing procedure applied involved preparing the acrylic casing, putting the large cutting sample inside the casing, gluing the body with the two end caps together and placing in a large metallic vessel capable of holding all the samples and withstanding 220 °F and 1000 psig and kept at a back pressure of 1000 psig. Pressure was then applied by pumping hydraulic oil until 800 psig was reached. A strap heater was used to raise the temperature to 220 °F and the samples were left inside for 24 hours. After that the system was allowed to cool and the pressure was released slowly. Finally, the two end caps were machined off using a lathe machine. The final embedded large cutting size samples and all core plugs after being drilled off are shown in Figure 1.

CT-scanning and heterogeneity parameters

A Ceretom NL 3000 multi-slice CT-scanner was used at relatively high X-ray energies (typically 140 kV, 7 mA) to generate the 2-D cross-sectional images every 1.25 mm both for the six selected core plugs before all experiments listed above, and for the large cutting size samples after the encasing process. The CTN (usually the mean CT or Hounsfield number for each slice) were converted to bulk densities (also called pseudo-bulk density, PBD) and porosities obtained from CT responses of known bulk density 'standards' which are scanned in a similar environment as the cores using the following equations:

$$PBD = CTN * m + c \quad (1)$$

$$\phi = (\rho_{ma} - PBD) / (\rho_{ma} - \rho_f) \quad (2)$$

The heterogeneity of the plug samples was classified according to their intra-slice and inter-slice CTNs. The intra-slice heterogeneity can be calculated by dividing the standard deviation of CTN by the mean CTN for each slice. This parameter (Std. dev./Mean) is also called the C_v , which is a measure of static heterogeneity. A higher average C_v in a sample represents overall higher intra-slice heterogeneity. The inter-slice heterogeneity, designated by Heterogeneity Index, HI, is calculated by dividing the maximum of the average CTN value for any slice within the sample by the minimum of the average CTN for all other slices. The higher this HI value, the higher the inter-slice heterogeneity. Finally, the Composite Heterogeneity Index, CHI, a new parameter introduced, is the product of the average C_v for a plug, the H.I., and a scaling factor of 10. In other words,

$$CHI = 10 * HI * C_v \quad (3)$$

CT-based relative permeability measurement procedure

Two types of experimental data curves (differential pressure curve and recovery curve) are required for the unsteady-state relative permeability measurement. Although differential pressure can be recorded very accurately during such a test, the uncertainty is too high for the recovery curves for the large cutting size samples which have very low pore volumes. Therefore, a steady-state technique involving in-situ saturation measurements with the help of CT was used. For instance, a large cutting sized Berea sandstone sample SST02AB, chosen for relative permeability measurement, was CT-scanned at 1.25 mm intervals with the total coverage 10 mm before and after it was vacuum saturated with the 5% by weight sodium iodide brine. The vacuum-saturated core provided one of the reference lines representing 100% water saturation (S_w). Soltrol-130 (the oil phase) was then injected to bring the sample to irreducible water saturation (S_{wir}), which gave the other reference line needed for in-situ saturation calculation. The S_{wir} is independently calculated by dividing the volume of produced brine phase by the pore volume of the sample. After that, oil and water at different fractional flows of water (f_w), (e.g. f_w set at 20%, 40%, 50%, and 100%) were injected until steady-state was reached (observed with pressure and flow stabilization). The differential pressure was then recorded and the sample was CT-scanned at the same eight slice locations to obtain the CT numbers corresponding to each fractional flow stage.

RESULTS AND DISCUSSIONS

Porosity and absolute permeability

The left part of Figure 3 shows the original core plugs were plotted against CT-derived porosities for all seventeen cutting size samples. For instance, the core plug SST02 has three points for which the y-axis shows the porosity of SST02 and the x-axis shows the porosity of each of its cutting size samples (*i.e.*, SST02H, SST02AB and SST02AT). Three points denoted by squares (for SST01) adjacent to each other are very close to the $y=x$ dotted line than other core plugs' points, which means SST01 is very homogenous (similarly for SST02's points in this plot). The cross-plot on the right presents a similar conclusion for SST02 in terms of absolute permeabilities. On the other hand the data (shown with the asterisk symbol) for LST01 for both porosity and permeability show the broadest distribution in the x-axis for a given y-axis value. This is followed by the points corresponding to samples DOL03 and DOL01. Four thin section images representing DOL01, DOL02, DOL03 and LST01 are shown in Figure 2. Among these, LST01 shows more variations in pore structure and geometry. An *ImageJ*-based segmentation technique was applied to calculate the porosity for two images for the two end pieces of each core plug. The porosity values derived this way for DOL01, DOL02, DOL03 and LST01 are 0.155, 0.148, 0.12, and 0.15, which is a reasonable match for the porosity values of the original core plugs which are 0.157, 0.152, 0.168, and 0.157, respectively.

Relative permeability data

Figure 5 shows eight CT-slices scanned when SST02AB was at S_{wir} , steady-state for four fractional flow stages corresponding to f_w of 20%, 40%, 80%, 100% during imbibitions and also at 100% brine saturation. As we can see from CT-slices of eight locations for 40% and 50%, the difference in saturation between 40% and 50% is not significant, which explained why the two curves almost fall on top of each other. A rainbow color scheme was used for the CTN range of 1300 to 1900 (the warmer the color, the higher the CT number). Within this imbibition cycle, we see clear increases in the CTNs (*i.e.* wetting-phase saturations), which were then plotted on the left-hand side of Figure 6. Together with the differential pressure data recorded for each stage; the final K_r curves of SST02AB were graphed on the right-hand side, together with unsteady-state K_r data of SST02 analysed using the JBN method. As we can see, K_{ro} and K_{rw} curves showed a not perfect match when considering unsteady-state only gave us parts of the relative permeability curves between the water saturation at the break-through and at PVIo. Also, steady-state permeability often differs from unsteady-state measurement, which explains why two curves differ in both magnitude and shape. Note that the $f_w=20\%$ fractional flow still had not reached steady-state when CT-scanned as had the other stages, because the water saturation at the outlet of SST02AB is still higher than that of the inlet. In this proposed procedure, SST02AB presents the length of 1.871 cm, diameter of 0.88cm, viscosity of 1.056 cp, which gives us a Rapoport and Leas [4] scaling factor ($LV\mu$) of about 1.6, when the flow rate is 0.5 cc/min. The capillary end effect can be ignored when the $LV\mu$ is more than 1.

Heterogeneity parameters

Based on the previous definition of heterogeneity parameters, we calculated the CHI for the six original core plugs and the seventeen large cutting size samples. The bar chart on the left-hand side of Figure 4 shows that there is a one-to-one correspondence in each orientation - AT, AB and H. For examples, in the H orientation, LST01H gives us the highest CHI, which is followed by DOL01, DOL02 and DOL03, and the other two Berea sandstones. Similar rankings were obtained for AT and AB orientations. Therefore, we quantitatively describe the LST01 as the most heterogeneous among the six core plugs based on CHI, whatever the size of the samples and orientations of large cutting size samples.

CONCLUSIONS

1. The permeability and porosity data shows a not bad match between large and small samples for Berea sandstone core plugs, even though not a perfect match in either shape or magnitude for the relative permeability. Due to the heterogeneity, no good agreement was observed for limestone and dolomite core plugs.
2. Three heterogeneity parameters were defined, and showed the potential to classify heterogeneity of rocks. CHI can be used to compare the heterogeneity in the sample selection process for special core analysis samples.

REFERENCES

- [1] Siddiqui, S., Grader, A.S., Touati, M., Loermans, A.M. and Funk, J.J.: "Techniques for Extracting Reliable Density and Porosity Data from Cuttings," SPE paper No. 96918, presented at the 2005 SPE Annual Technical Conference and Exhibition held in Dallas, Texas, 9-12 October 2005.
- [2] Lenormand, R., Bauget, F. and Ringot, G.: "Permeability measurement on small rock samples," presented at the International Symposium of the Society of Core Analysis held in Halifax, Nova Scotia, Canada, 4-7 October 2010.
- [3] Olafuyi, O.A., Cinar, Y., Knackstedt, M.A. and Pinczewski, W.V.: "Capillary Pressure and Relative Permeability of Small Cores," SPE 113386 presented at the SPE/DOE Improved Oil Recovery Symposium, Tulsa, Oklahoma, 19-23 April 2008.
- [4] Rapoport, L.A. and Leas, W.J.: "Properties of Linear Waterfloods", Trans., AIME (1953) Vol. 198, p. 28.

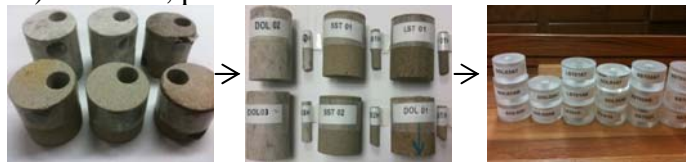


Figure 1. Resin encasing procedure and seventeen encased cutting size samples.

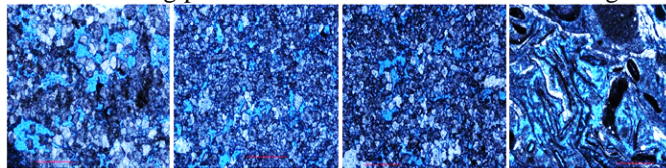


Figure 2. Four thin section images for DOL01, DOL02, DOL03 and LST01

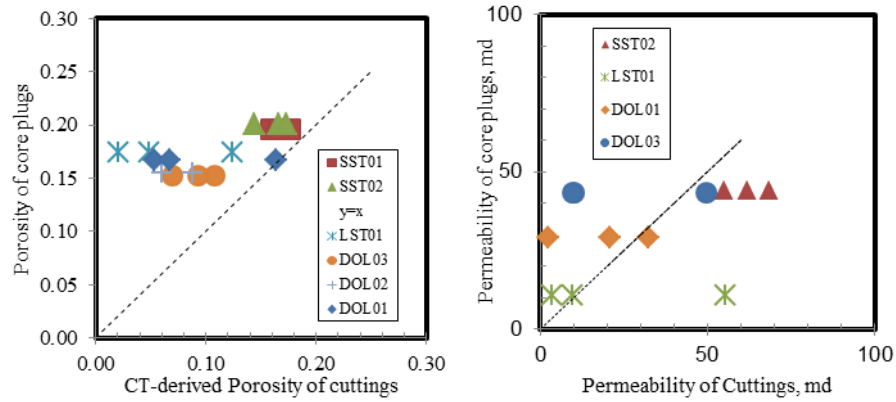


Figure 3. Cross-plots of K_a and Φ between core plugs and cutting size samples.

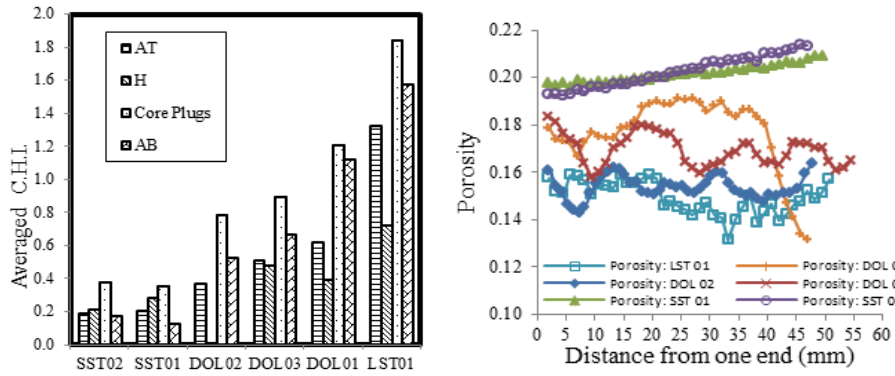


Figure 4. CHI bar chart and porosity distributions for six core plugs.

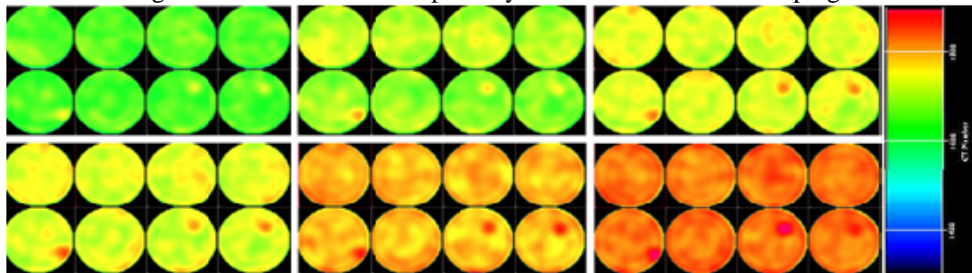


Figure 5. CT-slices for Swir, fw20, fw40, fw50, fw100 and 100% saturation

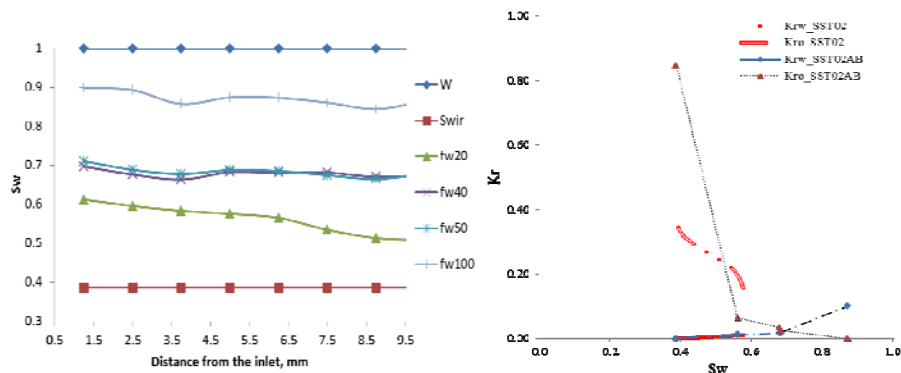


Figure 6. Saturation distributions and comparisons of K_r between SST02AB and SST02